

Fuzzy Logic Controller Based Single-Input Multiple-Output DC–DC Converter

Thrinnad Chokkakula

PG Student,
Department of Electrical and
Electronics Engineering,
ARTA Visakhapatnam,
Andhra Pradesh, India.

Ranadheer Inteti

Asst. Professor,
Department of Electrical and
Electronics Engineering,
ARTA Visakhapatnam,
Andhra Pradesh, India.

N Kiran Kumar

Asst. Professor,
Department of Electrical and
Electronics Engineering,
ARTA Visakhapatnam,
Andhra Pradesh, India.

Abstract:

The aim of this study is to develop a high-efficiency single-input multiple-output (SIMO) dc–dc converter. The proposed converter can boost the voltage of a low-voltage input power source to a controllable high-voltage dc bus and middle-voltage output terminals. Moreover, middle-voltage output terminals can supply powers for individual middle-voltage dc loads or for charging auxiliary power sources. In this study, a coupled-inductor based dc–dc converter scheme utilizes only one power switch with the properties of voltage clamping and soft switching, and the corresponding device specifications are adequately designed. As a result, the objectives of high-efficiency power conversion, high step up ratio, and various output voltages with different levels can be obtained. A fuzzy controller is designed to reduce the ripples.

Keywords:

DC TO DC converter, PI controller, Fuzzy controller.

I. INTRODUCTION:

In Order to protect the natural environment on the earth, the development of clean energy without pollution has the major representative role in the last decade. By dealing with the issue of global warming, clean energies, such as fuel cell (FC), photovoltaic, and wind energy, etc., have been rapidly promoted. Due to the electric characteristics of clean energy, the generated power is critically affected by the climate or has slow transient responses, and the output voltage is easily influenced by load variations. Besides, other auxiliary components, e.g., storage elements, control boards, etc., are usually required to ensure the proper operation of clean energy.

For example, an FC-generation system is one of the most efficient and effective solutions to the environmental pollution problem. In addition to the FC stack itself, some other auxiliary components, such as the balance of plant (BOP) including an electronic control board, an air compressor, and a cooling fan, are required for the normal work of an FC generation system. In other words, the generated power of the FC stack also should satisfy the power demand for the BOP. Thus, various voltage levels should be required in the power converter of an FC generation system. In general, various single-input single-output dc–dc converters with different voltage gains are combined to satisfy the requirement of various voltage levels, so that its system control is more complicated and the corresponding cost is more expensive. The motivation of this study is to design a single-input multiple-output (SIMO) converter for increasing the conversion efficiency and voltage gain, reducing the control complexity, and saving the manufacturing cost.

II. SIMO CONVERTER:

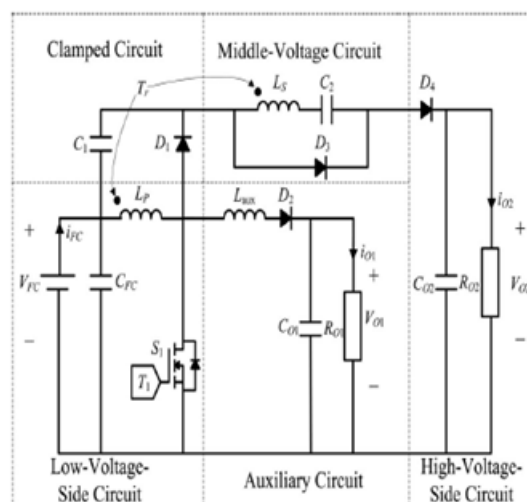


Fig 1. SIMO converter

In this paper presented a SIMO dc–dc converter capable of generating buck, boost, and inverted outputs simultaneously. However, over three switches for one output were required. This scheme is only suitable for the low output voltage and power application, and its power conversion is degenerated due to the operation of hard switching. Proposed a new dc–dc multi-output boost converter, which can share its total output between different series of output voltages for low- and high-power applications. Unfortunately, over two switches for one output were required, and its control scheme was complicated. Besides, the corresponding output power cannot supply for individual loads independently. Investigated a multiple-output dc–dc converter with shared zero-current switching (ZCS) lagging leg. Although this converter with the soft-switching property can reduce the switching losses, this combination scheme with three full-bridge converters is more complicated, so that the objective of high-efficiency power conversion is difficult to achieve, and its cost is inevitably increased.

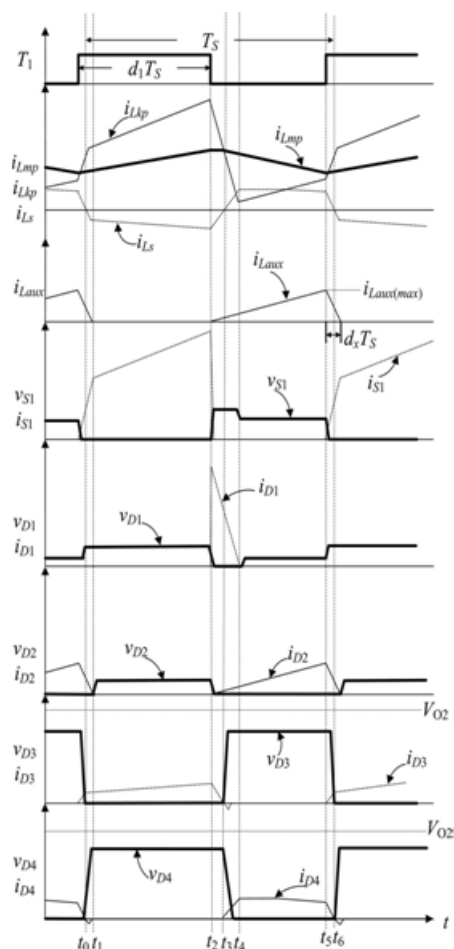


Fig 2 characteristics of proposed SIMO converter

Operating Modes

Mode 1 (t0-t1)

Mode 2 (t1-t2)

Mode 3 (t2-t3)

Mode 4 (t3-t4)

Mode 5 (t4-t5)

Mode 6 (t5-t6)

Operating Modes Explanation

MODE 1 (t0-t1)

In this mode, the main switch S_1 was turned ON for a span, and the diode D_4 turned OFF. Because the polarity of the windings of the coupled inductor Tr is positive, the diode D_3 turns ON. The secondary current i_{Ls} reverses and charges to the middle voltage capacitor C_2 . When the auxiliary inductor L_{aux} releases its stored energy completely, and the diode D_2 turns OFF, this mode ends.

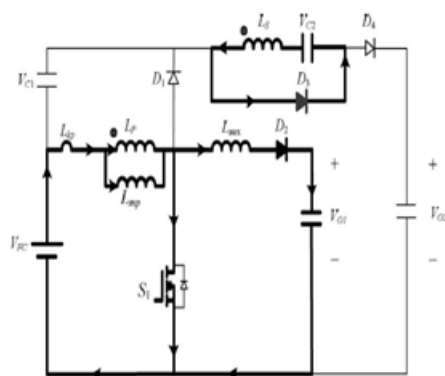


Fig2.1 operating mode (t0-t1)

MODE 2 (t1-t2):

At time $t = t_1$, the main switch S_1 is persistently turned ON. Because the primary inductor L_p is charged by the input power source, the magnetizing current i_{Lmp} increases gradually in an approximately linear way. At the same time, the secondary voltage v_{Ls} charges the middle-voltage capacitor C_2 through the diode D_3 .

Although the voltage v_{Lmp} is equal to the input voltage V_{FC} both at modes 1 and 2, the ascendant slope of the leakage current of the coupled inductor (di_{Lkp}/dt) at modes 1 and 2 is different due to the path of the auxiliary circuit. Because the auxiliary inductor L_{aux} releases its stored energy completely, and the diode D_2 turns OFF at the end of mode 1, it results in the reduction of di_{Lkp}/dt at mode 2.

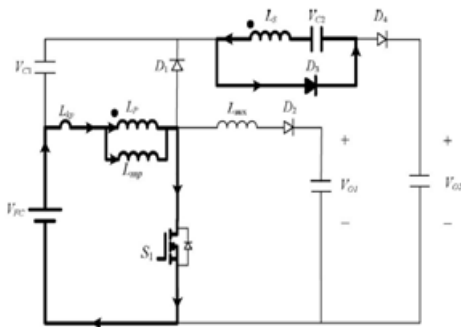


Fig2.2 operating mode (t1-t2)

MODE 3 (t2-t3):

At time $t = t_2$, the main switch S_1 is turned OFF. When the leakage energy still released from the secondary side of the coupled inductor, the diode D_3 persistently conducts and releases the leakage energy to the middle-voltage capacitor C_2 . When the voltage across the main switch V_{S1} is higher than the voltage across the clamped capacitor V_{C1} , the diode D_1 conducts to transmit the energy of the primary-side leakage inductor L_{kp} into the clamped capacitor C_1 . At the same time, partial energy of the primary-side leakage inductor L_{kp} is transmitted to the auxiliary inductor L_{aux} , and the diode D_2 conducts. Thus, the current $i_{L_{aux}}$ passes through the diode D_2 to supply the power for the output load in the auxiliary circuit. When the secondary side of the coupled inductor releases its leakage energy completely, and the diode D_3 turns OFF, this mode ends.

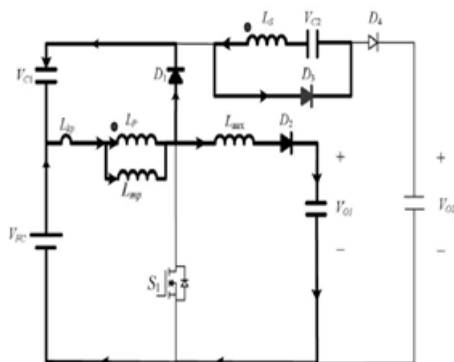


Fig2.3 operating mode (t2-t3)

MODE 4 (t3-t4):

At time $t = t_3$, the main switch S_1 is persistently turned OFF. When the leakage energy has released from the

primary side of the coupled inductor, the secondary current i_{LS} is induced in reverse from the energy of the magnetizing inductor L_{mp} through the ideal transformer, and flows through the diode D_4 to the HVSC. At the same time, partial energy of the primary-side leakage inductor L_{kp} is still persistently transmitted to the auxiliary inductor L_{aux} , and the diode D_2 keeps conducting. Moreover, the current $i_{L_{aux}}$ passes through the diode D_2 to supply the power for the output load in the auxiliary circuit.

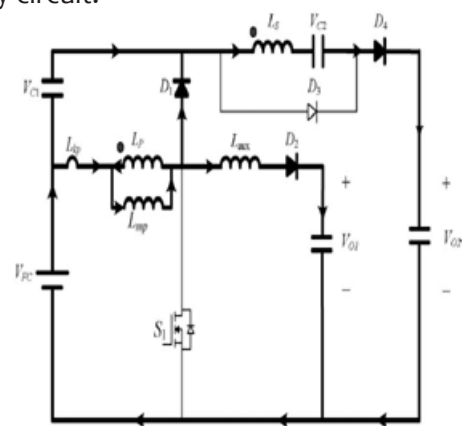


Fig2.4 operating mode (t3-t4)

MODE 5 (t4-t5):

At time $t = t_4$, the main switch S_1 is persistently turned OFF, and the clamped diode D_1 turns OFF because the primary leakage current $i_{L_{kp}}$ equals to the auxiliary inductor current $i_{L_{aux}}$. In this mode, the input power source, the primary winding of the coupled inductor T_r , and the auxiliary inductor L_{aux} connect in series to supply the power for the output load in the auxiliary circuit through the diode D_2 . At the same time, the input power source, the secondary winding of the coupled inductor T_r , the clamped capacitor C_1 , and the middle voltage capacitor (C_2) connect in series to release the energy into the HVSC through the diode D_4 .

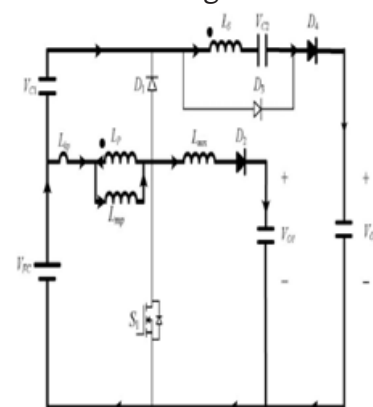


Fig2.5 operating mode (t4-t5)

MODE 6 (t5-t6):

At time $t=t_5$, this mode begins when the main switch S_1 is triggered. The auxiliary inductor current $i_{L_{aux}}$ needs time to decay to zero, the diode D_2 persistently conducts. In this mode, the input power source, the clamped capacitor C_1 , the secondary winding of the coupled inductor Tr , and the middle-voltage capacitor C_2 still connect in series to release the energy into the HVSC through the diode D_4 . Since the clamped diode D_1 can be selected as a low-voltage Schottky diode, it will be cut off promptly without a reverse-recovery current. Moreover, the rising rate of the primary current $i_{L_{kp}}$ is limited by the primary-side leakage inductor L_{kp} . Thus, one cannot derive any currents from the paths of the HVSC, the middle-voltage circuit, the auxiliary circuit, and the clamped circuit. As a result, the main switch S_1 is turned ON under the condition of ZCS and this soft-switching property is helpful for alleviating the switching loss. When the secondary current i_{LS} decays to zero, this mode ends. After that, it begins the next switching cycle and repeats the operation in mode 1.

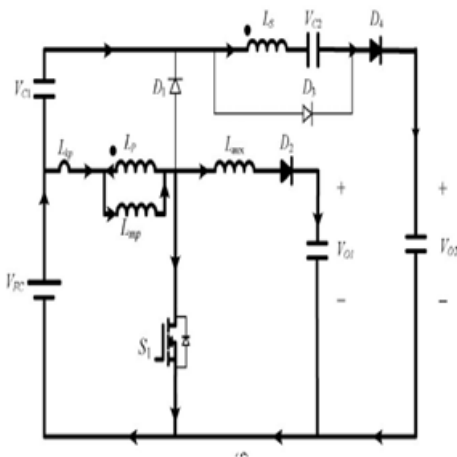


Fig2.6 operating mode (t5-t6)

III. FUZZY SYSTEM:

The fuzzy interface system Fuzzy system basically consists of a formulation of the mapping from a given input set to an output set using Fuzzy logic. The mapping process provides the basis from which the interference or conclusion can be made. A Fuzzy interface process consists of following steps .

Step 1: Fuzzification of input variables.

Step 2: Application of Fuzzy operator.(AND, OR, NOT) In the IF (antecedent) part of the rule.

Step 3: Implication from the antecedent to the consequent (Then part of the rule).

Step 4: Aggregation of the consequents across the rules.

Step 5: Defuzzification.

Generally there will be a matrix of rules similar to the ES rule matrix for Ex: There are 7MF for input variables 'x' and MF for input variable 'y' then there will be all together 35 rules.

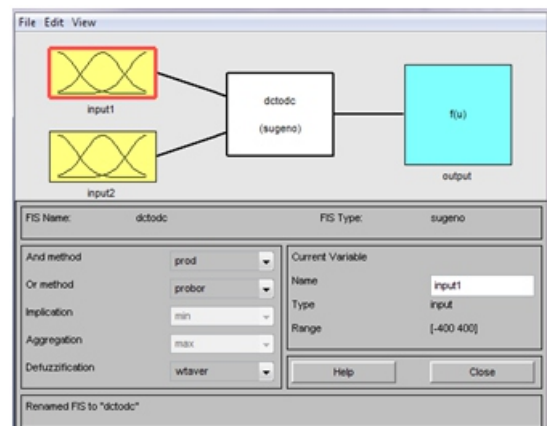


Fig2.6 Fuzzy controller

IV. SIMULATION DESIGN:

A simulation design open loop system as shown in Fig.4.1 is implemented in MATLAB SIMULINK with the help of coupled inductor, voltage clamping circuit and switched capacitor we get desired output voltage level (Fig.4.2 and Fig.4.3) low voltage output and high voltage waveforms, A modified circuit of the system with single phase inverter is also designed which is shown in Fig.4.4. the inverter output is also shown in fig4.5.

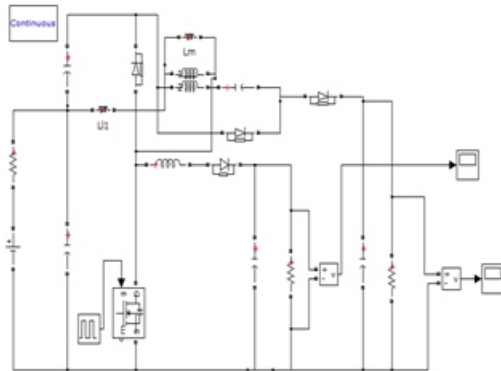


Fig.4.1. open loop system of SIMO Converter

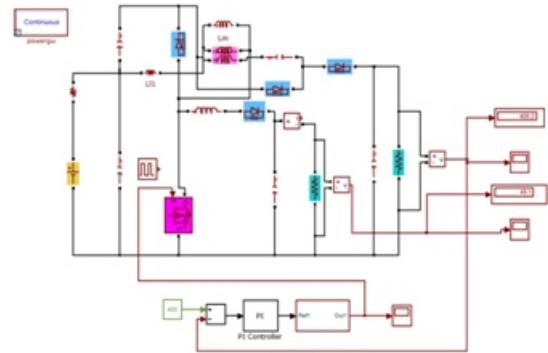


Fig.4.4. closed loop circuit of SIMO Converter with pi controller

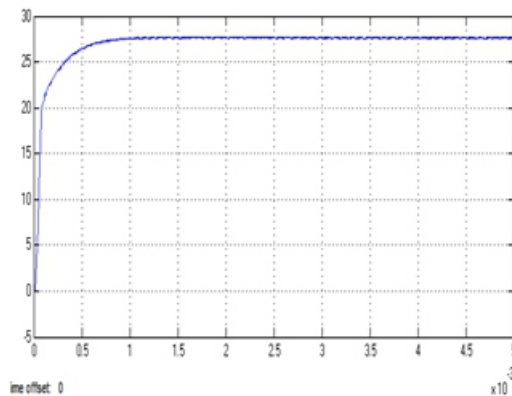


Fig.4.2. Low Voltage Output(28V DC)

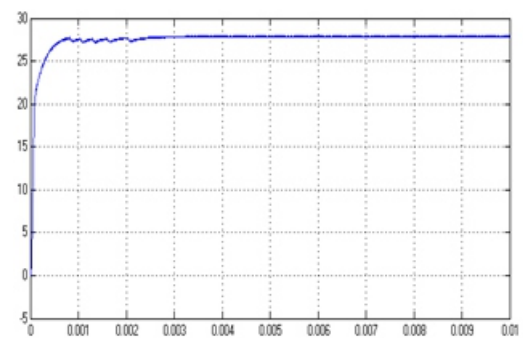


Fig.4.5. low voltage output (28V)

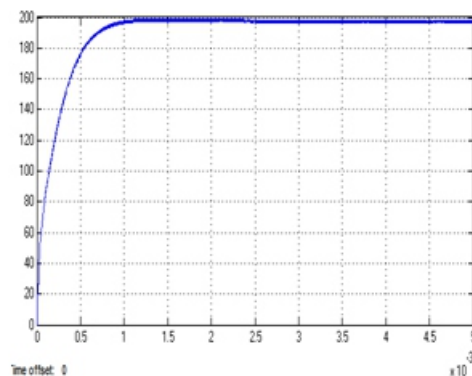


Fig.4.3. High voltage output(200V DC)

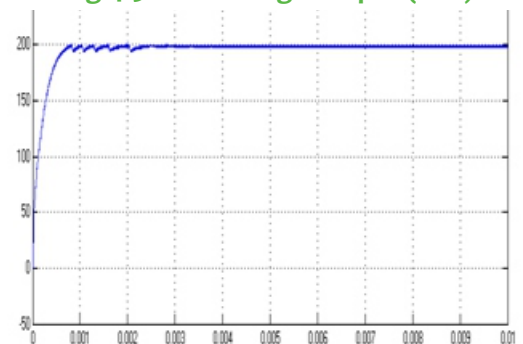


Fig.4.6. high voltage (200V)

A simulation design closed loop system as shown in Fig.4.4 is implemented in MATLAB SIMULINK with the help of coupled inductor, voltage clamping circuit and switched capacitor and PI controllers we get desired output voltage level (Fig.4.5 to Fig4.6) low voltage output and high voltage waveforms, A modified circuit of the system with single phase inverter is also designed which is shown in Fig4.7. the inverter output is also shown in fig4.8.

A simulation design closed loop system as shown in Fig.4.7 is implemented in MATLAB SIMULINK with the help of coupled inductor, voltage clamping circuit and switched capacitor and FUZZY controllers we get desired output voltage level (Fig.4.8 to Fig4.9) low voltage output and high voltage waveforms.

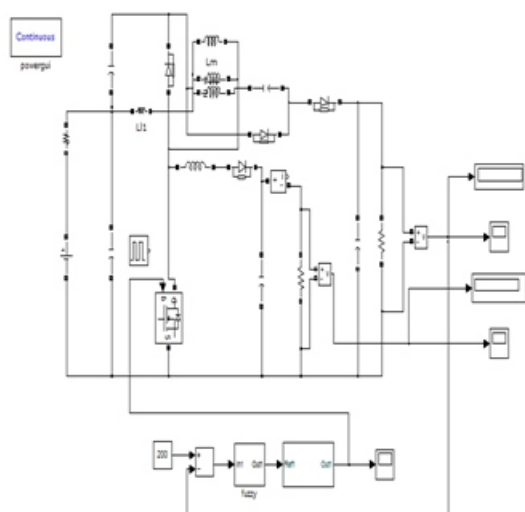


Fig.4.7. closed loop circuit of SIMO Converter with fuzzy controller

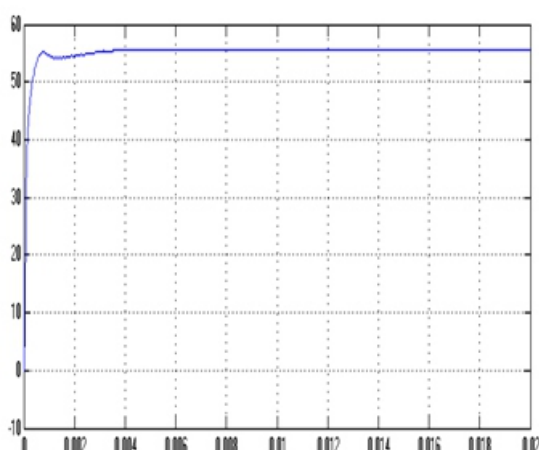


Fig.4.8. low voltage output (58V)

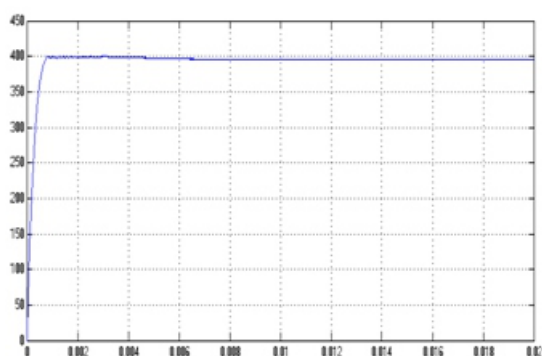


Fig.4.9. high voltage (400V)

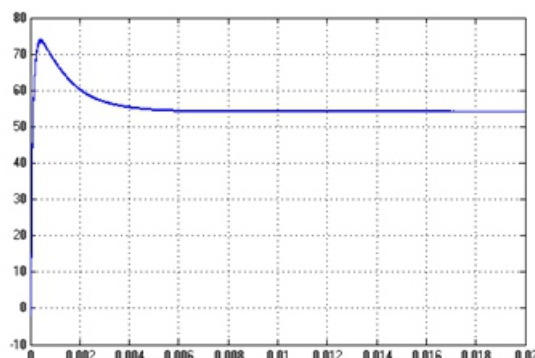


Fig.4.10. voltage across clamping circuit

V. CONCLUSION:

This project consists of a high-efficiency SIMO dc-dc converter, and this coupled-inductor-based converter was applied well to a single-input power source plus two output terminals composed of an auxiliary battery module and a high-voltage dc bus. The input to the converter is given by a solid oxide fuel cell. The controllers used are a PI controller and fuzzy controller. The results obtained by using PI controller are compared with fuzzy logic controller. The ripple content is reduced by using fuzzy logic controller. The results are verified using MATLAB software.

REFERENCES:

- [1] A. Kirubakaran, S. Jain, and R. K. Nema, "DSP-controlled power electronic interface for fuel-cell-based distributed generation," *IEEE Trans. Power Electron.*, vol. 26, no. 12, pp. 3853–3864, Dec. 2011.
- [2] B. Liu, S. Duan, and T. Cai, "Photovoltaic dc-building-module-based BIPV system-concept and design considerations," *IEEE Trans. Power Electron.*, vol. 26, no. 5, pp. 1418–1429, May 2011.
- [3] M. Singh and A. Chandra, "Application of adaptive network-based fuzzy interference system for sensorless control of PMSG-based wind turbine with nonlinear-load-compensation capabilities," *IEEE Trans. Power Electron.* vol. 26, no. 1, pp. 165–175, Jan. 2011.
- [4] C. T. Pan, M. C. Cheng, and C.M. Lai, "A novel integrated dc/ac converter with high voltage gain capability for distributed energy resource systems," *IEEE Trans. Power Electron.*, vol. 27, no. 5, pp. 2385–2395, May 2012.

[5] S. D. Gamini Jayasinghe, D. Mahinda Vilathgamuwa, and U. K. Madawala, "Diode-clamped three-level inverter-based battery/supercapacitor direct integration scheme for renewable energy systems," *IEEE Trans. Power Electron.*, vol. 26, no. 6, pp. 3720–3729, Dec. 2011.

[6] H. Wu, R. Chen, J. Zhang, Y. Xing, H. Hu, and H. Ge, "A family of threeport half-bridge converters for a stand-alone renewable power system," *IEEE Trans. Power Electron.*, vol. 26, no. 9, pp. 2697–2706, Sep. 2012.

[7] M. W. Ellis, M. R. Von Spakovsky, and D. J. Nelson, "Fuel cell systems: Efficient, flexible energy conversion for the 21st century," *Proc. IEEE*, vol. 89, no. 12, pp. 1808–1818, Dec. 2001.

[8] T. Kim, O. Vodyakho, and J. Yang, "Fuel cell hybrid electronic scooter," *IEEE Ind. Appl. Mag.*, vol. 17, no. 2, pp. 25–31, Mar./Apr. 2011.

[9] F. Gao, B. Blunier, M. G. Simões, and A. Miraoui, "PEM fuel cell stack modeling for real-time emulation in hardware-in-the-loop application," *IEEE Trans. Energy Convers.*, vol. 26, no. 1, pp. 184–194, Mar. 2011.

[10] P. Patra, A. Patra, and N. Misra, "A single-inductor multiple-output switcher with simultaneous buck, boost and inverted outputs," *IEEE Trans. Power Electron.*, vol. 27, no. 4, pp. 1936–1951, Apr. 2012.

[11] A. Nami, F. Zare, A. Ghosh, and F. Blaabjerg, "Multiple-output DC–DC converters based on diode-clamped converters configuration: Topology and control strategy," *IET Power Electron.*, vol. 3, no. 2, pp. 197–208, 2010.

[12] Y. Chen, Y. Kang, S. Nie, and X. Pei, "The multiple-output DC–DC converter with shared ZCS lagging leg," *IEEE Trans. Power Electron.*, vol. 26, no. 8, pp. 2278–2294, Aug. 2011.